

ORIGINAL ARTICLE

The effect of hydrogen gas evolution of magnesium implant on the postimplantation mortality of rats



Deni Noviana ^{a,**}, Devi Paramitha ^{a,b},
Mokhamad Fakhrol Ulum ^a, Hendra Hermawan ^{b,*}

^a Faculty of Veterinary Medicine, Bogor Agricultural University, Bogor, Indonesia

^b Department of Mining, Metallurgical and Materials Engineering & CHU de Québec Research Centre, Laval University, Quebec City, Canada

Received 12 May 2015; received in revised form 16 July 2015; accepted 3 August 2015

Available online 20 August 2015

KEYWORDS

biodegradable metal;
hydrogen evolution;
magnesium;
rat;
survival rate

Summary *Background/Objective:* Hydrogen gas cavity is formed during *in vivo* degradation of magnesium implants. In many studies, the gas cavity is mostly punctured out subcutaneously. However, this procedure becomes inapplicable in certain internal surgeries; therefore, the effect of this gas cavity is worth further assessment.

Methods: In this study, we investigated the effect of hydrogen gas evolution on the mortality of rats and analysed the whole body capacity to relieve the gas. Porous pure-magnesium implants were implanted in the femoral bone defect of adult Sprague-Dawley rats up to 18 days, and their survival rate was calculated while the gas cavity size was measured, and its effect was analysed with support of radiographic and blood analysis.

Results: The gas cavity was rapidly formed surrounding the implantation site and obviously decreased the rats' survival rate. The gas was observed to swell the surrounding implantation site by filling the loose compartments and then dispersing subcutaneously to other areas.

Conclusion: The rat's whole body capacity was unable to tolerate the rapid and persistent hydrogen gas cavity formation as shown by high postimplantation mortality.

Copyright © 2016, The Authors. Published by Elsevier (Singapore) Pte Ltd. This is an open access article under the CC BY-NC-ND license (<http://creativecommons.org/licenses/by-nc-nd/4.0/>).

* Corresponding author. Department of Mining, Metallurgical and Materials Engineering & CHU de Québec Research Centre, Laval University, 1065 ave. de la Médecine, Quebec City G1V 0A6, Canada.

** Corresponding author. Faculty of Veterinary Medicine, Bogor Agricultural University, Jl. Agatis Kampus Dramaga, Bogor 16680, Indonesia. E-mail addresses: deni@ipb.ac.id (D. Noviana), hendra.hermawan@gmn.ulaval.ca (H. Hermawan).

Introduction

Magnesium and its alloys have been extensively studied as potential biodegradable metals for bone temporary implants [1–5]. Despite their proven suitable compatibility to bone tissue [6–8], the nature of magnesium degradation is associated with hydrogen gas evolution, which forms gas cavities in the surrounding implantation tissue [9,10]. Overall, magnesium degrades *in vivo* via the corrosion reaction: $\text{Mg} + 2\text{H}_2\text{O} \rightarrow \text{Mg}(\text{OH})_2 + \text{H}_2$, which shows that 1 g of pure magnesium produces about 1 L of hydrogen gas. Once the local hydrogen saturation of blood and tissues are exceeded, diffusion and solubility of hydrogen in local biological tissues are hindered. Hydrogen gas then accumulates in tissue cavities [6,11]. A study has shown that hydrogen was not the major composition of the gas cavity in mice [10]. Most animal implantation studies on magnesium implants dealt with this subcutaneous gas cavity by puncturing the gas out [6,12]. However, this procedure may not be applicable for certain internal surgeries such as intraosseous pins and endovascular stents.

A small gas cavity may have little effect on the body system, as this gas is quickly exchanged with the surrounding tissue [10], but the effect of excessive gas cavity is yet to be ascertained as it may be harmful. Excessive hydrogen gas evolution creates pressure that induces some mechanical disturbances of bone regeneration resulting in distinct callus formation [9]. After all, this gas cavity formation was the main reason for which magnesium was abandoned in early usage [3]. Therefore, this study aims to analyse the whole body capacity of rats to relieve hydrogen gas from a magnesium implant and to investigate the effect of hydrogen gas evolution on its mortality. Implants were made from sintered magnesium powders; thereby, their porous structure allows for a fast degradation and excessive hydrogen evolution. Gas cavity formation was observed under radiography and survival rate of the rats was calculated.

Materials and methods

Porous magnesium implant preparation

Closed-porous pure magnesium implants (diameter 13 mm, thickness 2.5 mm, weight 0.24–0.26 g, porosity <5%) were prepared via powder sintering process. Commercial purity pure magnesium powders (< 100 μm) were uniaxially pressed under 13.8 MPa into tablets, and then sintered under argon at 400 °C for 1 hour and cooled to room temperature. The sintered tablets (implants) were sterilised with a hot dry air oven at 160 °C and UV light for 60 minutes prior to implantation. Detailed characterisation and testing of the material were not performed as they are not the focus of this study.

Animal preparation and implantation procedure

Twenty adult Sprague-Dawley rats (weight 147 ± 10 g, age 12 weeks) were used in this study with ethical clearance from the Animal Care and Use Ethics Committee of Bogor

Agricultural University (ACUC No: 6-2014 IPB). The implant weight accounted for ~1.7% of the rat's weight, which can be considered high. All rats were acclimatized for 2 weeks before the study with oral administration of acclimatization drugs with 10 mg/kg antibiotic (Claneksi, PT. Sanbe Farma, Jakarta, Indonesia) for 5 days, 10 mg/kg anthelmintic (Univerm, VMD, Budapest, Hungary) twice before and after antibiotic administration, and 20 mg/kg antiprozoa (Flagyl, Oubari Pharma, Damascus, Syria) for 5 days. All rats were anaesthetised intraperitoneously by using 50 mg/kg of ketamin hydrochloric acid combined with 5 mg/kg of xylazine hydrochloric acid (Ilium, Troy Laboratories, Glendenning, Australia). Right lateral femoral hair were then clipped and disinfected by using 70% alcohol and 10% povidone iodine prior to surgery. The skin was incised and the femoral muscle was retracted until the femur bone reached. The implant was inserted into flatten bone defects drilled at the femur bone on latero-medial region. The sham group was treated with the same surgical procedure but without implantation of magnesium and thus served as the control group. Femoral muscle and skin were then sutured by using 5/0 synthetic absorbable polyglactin suture (Hinglact, HiCare, Kerala, India).

Postimplantation observation and analysis

Death of the rats was noted and a survival rate was calculated in term of percent mortality up to Day 18 post-implantation. Body swelling as an indication of gas cavity formation was directly measured by using a calliper for its length in longitudinal and transversal directions (in cm) throughout the implantation period. The gas cavity was also observed by using a portable digital computer radiography (CR7 Vet Digital X-Ray, iM3 Inc., USA) at Day 7 and Day 14 postimplantation. Radiodensity was further analysed with the help of an image analysis software (ImageJ, NIH, USA). Peripheral blood profile was monitored before implantation and at Day 7 postimplantation by collecting 0.5 mL blood sample from the tail venous of each rat and placing in ethylenediaminetetraacetic acid vacutainer for blood parameters analysis. Statistical analysis was done by using a one-way analysis of variance with a post hoc Duncan test using SPSS v.16.0 software (SPSS Inc., USA) at a 95% confidence level. A value of $p < 0.05$ was considered as statistically significant.

Results

Figure 1 shows the magnesium tablet implantation process, survival rate curves, and gas cavity formation. Gas cavity was rapidly formed around the implantation site and obviously visible. A smooth skin bulging was observed and the skin palpation produced sensation of gas cavity during observation time at Day 7 postimplantation (Figures 1C and 1D). The number of survived rats was rapidly decreasing with no survival at Day 18 postimplantation.

Figure 2 shows the size of gas cavities and its distribution in different part of the rat's body measured throughout the implantation period. The gas cavity size reached its maximum at Day 5 and was decreasing in the following implantation days (Figure 2A). The gas cavity was spreading

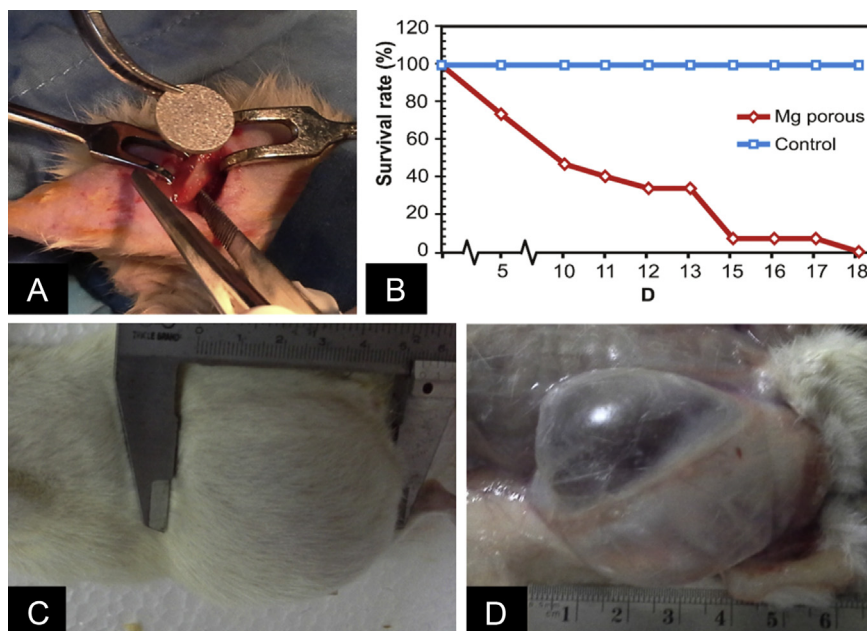


Figure 1 (A) Implantation process; (B) survival rate of the group of rats with magnesium implants ($n = 15$) compared with sham group ($n = 5$); (C) gas cavity at the medial area; and (D) subcutaneous opening of the medial area at Day 7 postimplantation. Mg = magnesium.

from the tight compartment (muscle) to the entire loose compartments (subcutaneous) such as caudal, medial, and lateral zone of the femoral region and then the ventral and dorsal zone of the rat's body (Figure 2B).

Figure 3 shows radiograms of the gas cavities in the rat's body at Day 7 and Day 14 postimplantation, where their size is not different for both periods. The gas cavity appears as black in colour (radiolucent), muscle is seen as more white (radiopaque), and bone is highly radiopaque, as commonly seen [13], while the magnesium implants appears as radiopaque as bone. Spreading of gas cavity from muscular to subcutaneous region is clearly shown in Figures 3B and 3C. More loose compartments were filled by the gas as implantation time prolonged as observed in the dorsal- and ventral-body regions (Figure 3D). The gas cavity size was further decreased up to Day 18 due to rupture (Figure 3E).

Figures 4 and 5 show radiograms and its further analysis of the bone defect of both the magnesium implant group and the sham group. The healing of bone defect is not clearly seen on the sham group compared with magnesium

implant group (Figures 4A–4C). The radiodensity of bone defects in both groups decrease at Day 14 and then slightly increase at Day 17 postimplantation (Figure 5A), but not statistically significant ($p > 0.05$). Meanwhile, the healing progress in the magnesium group was well observed from different radiopacities which were higher on Day 14 than Day 7 and Day 17 postimplantation (Figures 4D–4F). The radiodensity of the bone defect in magnesium group decreased at Day 14 and increased at Day 17 postimplantation (Figure 5B) with statistical significance ($p < 0.05$).

Table 1 presents a peripheral blood profile of the rats before and after 7 days implantation, where certain blood parameters such as haemoglobin (Hb), packed cell volume (PCV), agranulocyte, granulocyte, lymphocyte, neutrophil, and neutrophil/lymphocyte ratio ratio are significantly different for both groups ($p < 0.05$). The value of Hb, PCV, agranulocyte, and lymphocyte decreased while only granulocyte increased after 7 days implantation. Meanwhile, there is no different for other parameters such as red blood

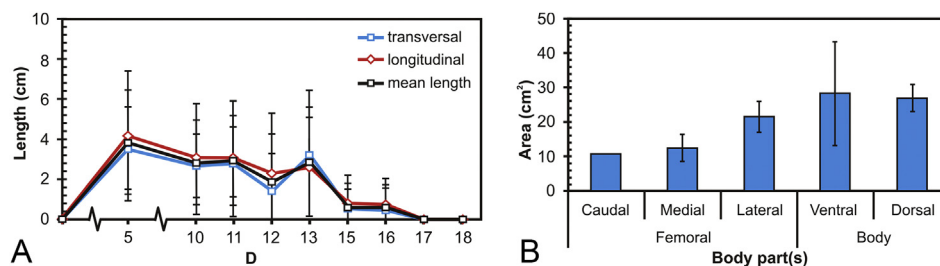


Figure 2 (A) Gas cavity size evolution throughout the implantation period; and (B) gas cavity size at different parts of the rat's body. Note: size was approximated by measuring longitudinal and transversal lengths of the gas cavities, and area was calculated by multiplying the measured lengths.

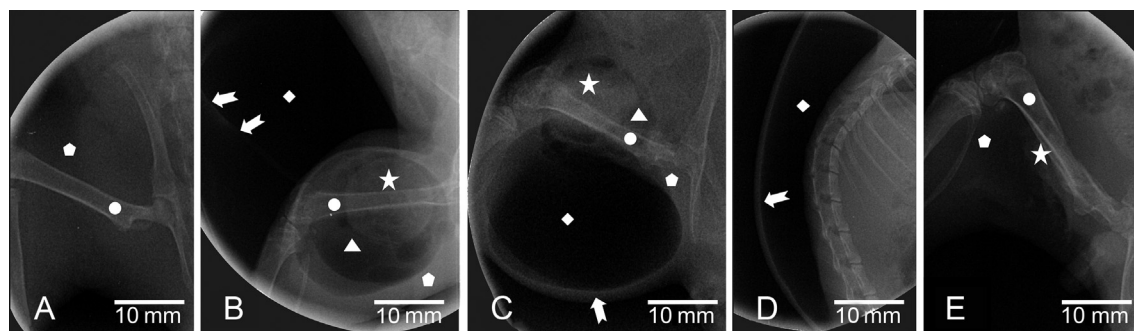


Figure 3 Radiograms of: (A) sham group, and gas cavity in the magnesium implant group at: (B) medial/lateral and cranial of femoral area at Day 7 postimplantation, (C) caudal of femoral area; (D) dorsal body area in lateral view at Day 14 postimplantation, and (E) gas cavity rupture at Day 17 post-implantation. Arrow = outer line of subcutaneous gas cavity; Circle = femur bone; Diamond = subcutaneous gas cavity; Pentagon = muscle; Star = implant; Triangle = intramuscular gas cavity.

cells (RBC), mean corpuscular volume, mean corpuscular haemoglobin, mean corpuscular haemoglobin concentration, white blood cells, monocyte, eosinophil, and basophil ($p > 0.05$).

Discussion

Gas cavity was rapidly formed once the implantation procedure was completed, indicating instantaneous reaction of magnesium implant with the body fluid where hydrogen gas is produced. The produced gas was then distending into the surrounding implantation tissues and caused massive soft tissue (muscle and subcutaneous) emphysema. In fact, the gas can be removed easily by using a needle or syringe inserted subcutaneously as commonly practiced [6,12]. However, that was not performed in this study as we had aimed to observe the effect of gas evolution to the survival rate of the rats. Evidently, it was shown that the rat's body

tolerance to the gas cavity was compromised resulting into a decrease of its survival rate (Figure 1). The produced gas throughout the implantation period, as the corrosion reaction of magnesium implant continued, made the gas cavity persistent, distracted muscle tissue, and spread into looser subcutaneous compartments (Figures 2, 3) and this was not well tolerated by the rat's body system. The massive tissue emphysema caused discomfort to the rats which in turn affected their bioactivity toward activities important for survival, such as getting nutrients. It is known that the body responses systematically to discomfort via disturbances of body fluid and cells expressed by the organs function. Similar subcutaneous emphysema was reported to occur as an adverse effect of carbon dioxides absorption during laparoscopic surgery procedure [14,15]. A non-extensive subcutaneous emphysema during laparoscopy surgery has obliged patients to take 2–3 days for recovery [14].

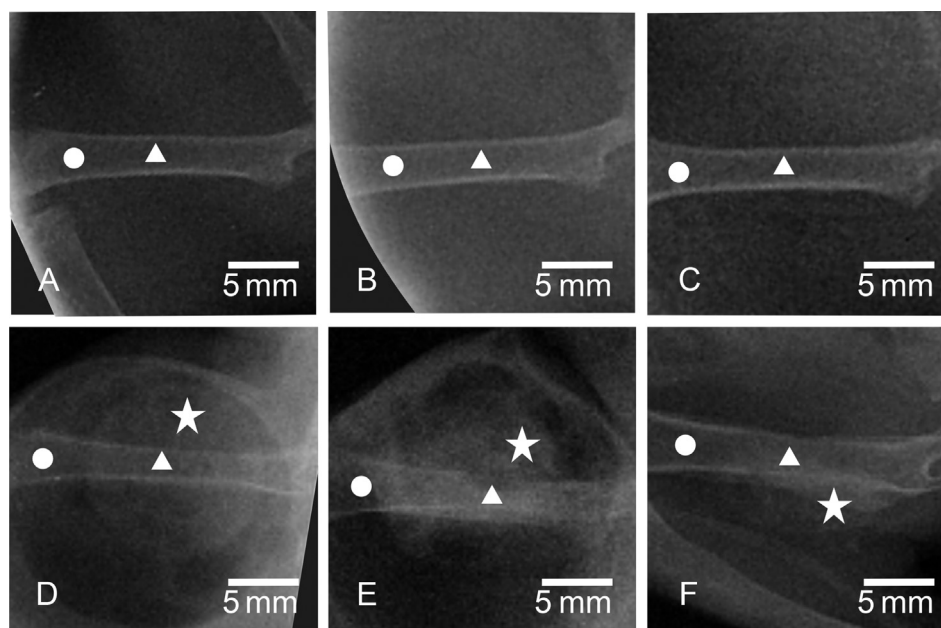


Figure 4 Radiograms of sham group at: (A) Day 7; (B) Day 14; (C) Day 17 postimplantation, and magnesium implant group at: (D) Day 7; (E) Day 14; (F) Day 17 postimplantation. Circle = femur bone; star = implant; triangle = bone defect area.

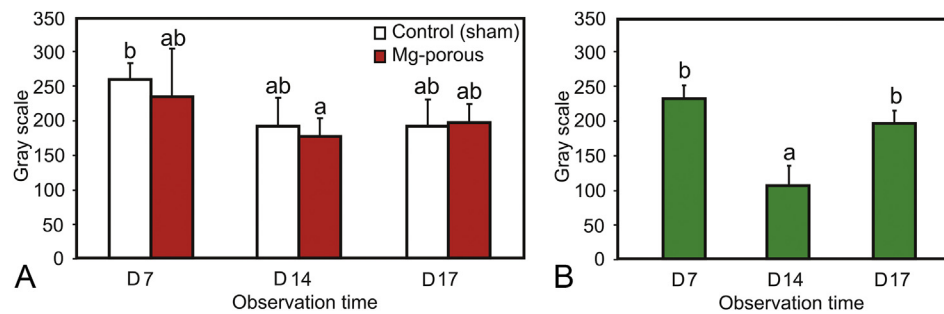


Figure 5 Radiodensity analysis of: (A) bone defect; and (B) magnesium implant on different days postimplantation. Note: The same letter above different bars indicates the difference is not significant ($p > 0.05$). Mg = magnesium.

Systemic body response, as observed from the changes in peripheral blood parameters (Table 1), showed a decrease of Hb count and PCV at Day 7 postimplantation. The decrease of RBC is, however, not statistically significant. The decrease of Hb and PCV indicates that presence of hydrogen gas in the surrounding soft tissue influences RBC functionality. The gas cavity induced discomfort and prolonged pain to the rat and influenced food intake, which in turn affected blood cells formation. The hydrogen gas in tissue emphysema influences gas exchange in blood, especially affects Hb [16]. Hydrogen ions have the tendency to diffuse into the blood from the interstitial fluid where Hb in RBC then buffers the ions. The Hb changes its shape after binding to additional hydrogen ions causing oxygen release, then picks up carbon dioxide to be released in the lungs [17]. In tolerable levels, hydrogen gas is fastly exchanged from the cavity into the surrounding tissue [10, 18] and the body is more sensitive to change in hydrogen concentration, estimated 100,000 times, than to change in potassium concentration [19]. The control of hydrogen ion concentration is done within seconds by the buffer systems and within minutes by the excretion of carbon dioxide via expiration in the

lungs, then within hours to days by excretion in the kidney, and reabsorption of carbonic acid [16]. However, massive tissue emphysema by hydrogen gas could lead to a severe disturbance of gaseous exchange in the tissue and the blood by appearing highly hydrogen gas for oxygen and carbon-dioxide transportation in the body [20].

Even though magnesium is the second most abundant element in the body and the second most common deficiency, disturbances in high level (hypermagnesemia) within the body are rare [21]. Excess of magnesium is directly excreted through kidney [19] and hypermagnesemia usually only occurs following renal failure. In contrast, hypomagnesemia is more common and the deficiency of magnesium may bring risk to mortality [22]. Magnesium hydroxide produced during degradation of magnesium and is deposited in the surrounding implantation tissue. It has low solubility in water, suggesting it is poorly absorbed in the digestive system [23]. The presence of this degradation product in the tissue triggers the arrival of inflammatory cells such as leukocyte and macrophage (Table 1). Neutrophil, a part of leukocyte cells, and macrophage cells release acid in form of H_2O_2 by

Table 1 Peripheral blood profile of rats before and after 7 days implantation.

Blood cell parameters	Preimplantation	7 d postimplantation		p
	All groups	Control	Mg-porous	
RBC (10^6 cells/ μ L)	10.3 \pm 1.5 ^a	8.3 \pm 1.2 ^a	7.8 \pm 3.1 ^a	0.122
Hb (g/dL)	13.6 \pm 1.2 ^b	12.4 \pm 1.1 ^b	9.9 \pm 2.3 ^a	0.004
PCV (%)	40.8 \pm 5.5 ^b	36.8 \pm 1.5 ^b	26.5 \pm 7.2 ^a	0.002
MCV (fL)	41.0 \pm 5.1 ^{ab}	44.9 \pm 5.1 ^b	35.2 \pm 6.0 ^a	0.062
MCH (pg)	13.6 \pm 1.0 ^a	15.0 \pm 1.1 ^a	13.3 \pm 2.5 ^a	0.240
MCHC (%)	33.6 \pm 4.6 ^a	33.6 \pm 1.9 ^a	37.7 \pm 1.6 ^a	0.184
WBC (10^3 cells/ μ L)	8.3 \pm 2.5 ^a	7.7 \pm 3.9 ^a	6.3 \pm 0.8 ^a	0.449
Agranulocyte (% WBC)	87.1 \pm 5.3 ^b	81.5 \pm 9.8 ^b	63.8 \pm 13.5 ^a	0.002
Lymphocyte (% WBC)	84.7 \pm 5.3 ^b	79.0 \pm 11.2 ^b	60.0 \pm 14.6 ^a	0.002
Monocyte (% WBC)	2.4 \pm 1.2 ^a	2.5 \pm 1.7 ^a	3.8 \pm 1.3 ^a	0.311
Granulocyte (% WBC)	12.9 \pm 5.3 ^a	18.5 \pm 9.8 ^a	36.3 \pm 13.5 ^b	0.002
Neutrophil (% WBC)	12.6 \pm 5.2 ^a	17.3 \pm 8.3 ^a	34.8 \pm 13.4 ^b	0.002
Eosinophil (% WBC)	0.3 \pm 0.5 ^a	1.3 \pm 1.9 ^a	1.5 \pm 0.6 ^a	0.127
Basophil (% WBC)	NIL	NIL	NIL	NIL
N/L	0.2 \pm 0.1 ^a	0.2 \pm 0.1 ^a	0.6 \pm 0.4 ^b	0.003

^{a,b} Description: data shown as mean with standard deviation ($x \pm$ standard deviation). The same letter in different rows indicates the difference is not significant ($p > 0.05$).

Hb = haemoglobin, L = lymphocyte; MCH = mean corpuscular haemoglobin; MCHC = mean corpuscular haemoglobin concentration; MCV = mean corpuscular volume; N = neutrophil; PCV = packed cell volume; RBC = red blood cells; WBC = white blood cells.

respiratory burst which in turn cuts off magnesium hydroxide bonding to be Mg^{2+} ion and H_2O [24]. However, the number of macrophage and its phagocytic capacity (efficiency) is limited in short period [25]. Therefore, the released Mg^{2+} ion concentration is limited at low level. Furthermore, the gas cavity might also act as barrier for tissue contact between cells and degradation product (Figure 3). A larger gas cavity creates greater distance for cells contact. Thus, hypomagnesaemia caused by the magnesium implant seems impossible and high mortality of rat in this study can be mostly related to the massive tissue emphysema.

The drilled bone (cortical bone defect) is suitable for bone-implant interface reaction analysis and this defect is able to self-induce bone tissue to heal from injury [26]. The presence of gas cavity influences this bone healing process as shown by more bone callus formed at the perimagnesium implant (Figure 4). This gas cavity created a loose tissue compartment causing magnesium tablet to move freely and induce friction at the bone defect surface. This friction induced more callus formation during bone healing process which was not seen on the sham group. An unfixed bone healing (unstable/moving) has been known to induce higher callus formation [26,27]. The gas cavity that filled muscle at loose peri-implant compartment decreases radiodensity (Figure 5A). In radiography, the presence of gas creates radiolucent as it has lower density compared with soft- and hard-tissues [13,28]. The change in radiodensity is a good indication of the biodegradation process of magnesium implants, as also observed for bioactive magnesium–calcium implants [29]. The deposited magnesium hydroxide on the magnesium implant surface and bone defect interface increased the radiodensity at Day 17 postimplantation (Figure 5B), even though it was decreasing at Day 14 postimplantation due to superimposition of gas with degradation product.

Table 1 also indicates that the rat's body cellular immunity was also disturbed by the presence of gas cavity. White blood cells and agranulocyte cells counts were decreased while granulocyte was increased. Granulocyte cells that react rapidly toward foreign body were present at prolonged days due to the incapability of agranulocyte cells to digest the magnesium due to the formed barrier between tissues (cells) and the surface of magnesium by the gas cavity (Figures 1, 3). This condition increased the tendency of high cellular stress as expressed by N/L ratio that is three times higher compared to those of control and preimplantation. Higher N/L ratio was also observed for other biodegradable implants, such as iron-bioceramic composite when compared to inert stainless steel implant [30]. Finally, it was shown that fast degradation of porous magnesium implant and high implant-body weight ratio created excessive gas cavity that compromised the normal body capacity to relieve the gas indicating the importance of controlling the degradation rate of magnesium implant as well as keeping a low implant-body weight ratio.

Conclusion

Our work has shown the adverse effect of excessive hydrogen gas evolution to the survival rate of rats

implanted with magnesium implants. The gas cavity spreads from muscle to more loose subcutaneous tissue and causes massive subcutaneous emphysema in the rat's body. The persistent presence of gas cavity causes prolonged discomfort and disturbs the balance of blood cell parameters which in turn decreases the survival rate. Excessive gas cavity resulted from magnesium implant degradation, therefore, should be seriously taken into consideration for the design of better magnesium implants and for their clinical translation.

Conflicts of interest

The authors have no conflicts of interest to declare.

Funding/support

The authors acknowledge the support of the Indonesian Ministry of Education and Culture-DGHE for the research grant (083/SP2H/PL/Dit.Litabmas/II/2015) and Laval University and CHU de Québec Research Centre for the fonds de demarrage.

Acknowledgements

The authors thank Ahmad Kafrawi Nasution and Abdul Hakim Yusop for their help during implant preparation.

References

- [1] Staiger MP, Pietak AM, Huadmai J, Dias G. Magnesium and its alloys as orthopedic biomaterials: a review. *Biomaterials* 2006;27:1728–34.
- [2] Witte F, Hort N, Vogt C, Cohen S, Kainer KU, Willumeit R, et al. Degradable biomaterials based on magnesium corrosion. *Curr Opin Solid State Mater Sci* 2009;12:63–72.
- [3] Witte F. The history of biodegradable magnesium implants: a review. *Acta Biomater* 2010;6:1680–92.
- [4] Zheng YF, Gu XN, Witte F. Biodegradable metals. *Mater Sci Eng R-Rep* 2014;77:1–34.
- [5] Luthringer BJ, Feyerabend F, Willumeit-Römer R. Magnesium-based implants: a mini-review. *Magn Res* 2014;27:142–54.
- [6] Witte F, Kaese V, Haferkamp H, Switzer E, Meyer-Lindenberg A, Wirth CJ, et al. *In vivo* corrosion of four magnesium alloys and the associated bone response. *Biomaterials* 2005;26:3557–63.
- [7] Witte F, Ulrich H, Rudert M, Willbold E. Biodegradable magnesium scaffolds: Part 1: appropriate inflammatory response. *J Biomed Mater Res A* 2007;81:748–56.
- [8] Witte F, Ulrich H, Palm C, Willbold E. Biodegradable magnesium scaffolds: Part II: peri-implant bone remodeling. *J Biomed Mater Res A* 2007;81:757–65.
- [9] Kraus T, Fischerauer SF, Hänzli AC, Uggowitzer PJ, Löffler JF, Weinberg AM. Magnesium alloys for temporary implants in osteosynthesis: *in vivo* studies of their degradation and interaction with bone. *Acta Biomater* 2012;8:1230–8.
- [10] Kuhlmann J, Bartsch I, Willbold E, Schuchardt S, Holz O, Hort N, et al. Fast escape of hydrogen from gas cavities around corroding magnesium implants. *Acta Biomater* 2013;9: 8714–21.

- [11] Witte F, Fischer J, Nellesen J, Vogt C, Vogt J, Donath T, et al. *In vivo* corrosion and corrosion protection of magnesium alloy LAE442. *Acta Biomater* 2010;6:1792–9.
- [12] Chaya A, Yoshizawa S, Verdelis K, Myers N, Costello BJ, Chou D-T, et al. *In vivo* study of magnesium plate and screw degradation and bone fracture healing. *Acta Biomater* 2015; 18:262–9.
- [13] Thrall DE. *Textbook of Veterinary Diagnostic Radiology*. The Netherlands: Elsevier Health Sciences; 2013.
- [14] Worrell J, Cleary D. Massive subcutaneous emphysema and hypercarbia: complications of carbon dioxide absorption during extraperitoneal and intraperitoneal laparoscopic surgery-case studies. *AANA J* 2002;70:456–62.
- [15] Ko M-L. Pneumopericardium and severe subcutaneous emphysema after laparoscopic surgery. *J Minim Invasive Gynecol* 2010;17:531–3.
- [16] Siggaard-Andersen O, Salling N. Oxygen-linked hydrogen ion binding of human haemoglobin. Effects of carbon dioxide and 2,3-diphosphoglycerate. II. studies on whole blood. *Scand J Clin Lab Invest* 1971;27:361–6.
- [17] Rao MS, Nagendranath V. Arterial blood gas monitoring. *Indian J Anaesth* 2002;46:289–97.
- [18] Harrison A-M. Acid-base physiology: the role of blood gases. *Biomed Sci* 2011;55:538–40.
- [19] Siggaard-Andersen O, Fogh-Andersen N. Base excess or buffer base (strong ion difference) as measure of a non-respiratory acid-base disturbance. *Acta Anaesthesiol Scand Suppl* 1995; 39:123–8.
- [20] Dash RK, Bassingthwaighe JB. Simultaneous blood–tissue exchange of oxygen, carbon dioxide, bicarbonate, and hydrogen ion. *Ann Biomed Engineering* 2006;34:1129–48.
- [21] Topf J, Murray P. Hypomagnesemia and hypermagnesemia. *Rev Endocr Metab Disord* 2003;4:195–206.
- [22] Soliman HM, Mercan D, Lobo SSM, Mélot C, Vincent J-L. Development of ionized hypomagnesemia is associated with higher mortality rates. *Crit Care Med* 2003;31:1082–7.
- [23] Coudray C, Rambeau M, Feillet-Coudray C, Gueux E, Tressol J, Mazur A, et al. Study of magnesium bioavailability from ten organic and inorganic Mg salts in Mg-depleted rats using a stable isotope approach. *Magnes Res* 2005;18:215–23.
- [24] Iles K, Forman H. Macrophage signaling and respiratory burst. *Immunol Res* 2002;26:95–105.
- [25] Zhidao X, James TT. A review on macrophage responses to biomaterials. *Biomed Mater* 2006;1:R1–9.
- [26] Shapiro F. Bone development and its relation to fracture repair: the role of mesenchymal osteoblasts and surface osteoblasts. *EurCells Mater* 2008;15:53–76.
- [27] Oryan A, Alidadi S, Moshiri A. Current concerns regarding healing of bone defects. *Hard Tissue* 2013;2:13.
- [28] Nomoto R, Mishima A, Kobayashi K, McCabe JF, Darvell BW, Watts DC, et al. Quantitative determination of radio-opacity: equivalence of digital and film X-ray systems. *Dent Mater* 2008;24:141–7.
- [29] Yu K, Chen L, Zhao J, Wang R, Dai Y, Huang Q. *In vivo* biocompatibility and biodegradation of a Mg-15%Ca₃(PO₄)₂ composite as an implant material. *Mater Lett* 2013;98:22–5.
- [30] Ulum MF, Nasution AK, Yusop AH, Arafat A, Kadir MRA, Juniantito V, et al. Evidences of *in vivo* bioactivity of Fe-bioceramic composites for temporary bone implants. *J Biomed Mater Res B Appl Biomater* 2015;103(7):1354–65. <http://dx.doi.org/10.1002/jbm.b.33315>.